Hindawi
Journal of Food Biochemistry
Volume 2024, Article ID 6245499, 16 pages
https://doi.org/10.1155/2024/6245499

Research Article

Dendrobium huoshanense Improves Lipid Metabolism Disorder by Restoring Gut Flora and Metabolites in Mice Fed a High-Fat Diet

Menghua Ma,[1,2,3] Fangli Gu,[1] Zongcui Yue,[1] Leilei Gao,[1] Chuangbo Chen,[1] Qiyan Lin,[1] Ke Huang,[1] Xiaoxue Li,[1] Jun Dai,[1] and Bangxing Han[1,2,3]

[1]*West Anhui University, Lu'an, China*
[2]*Traditional Chinese Medicine Institute of Anhui Dabie Mountain, West Anhui University, Lu'an, China*
[3]*Anhui Engineering Research Center for Eco-Agriculture of Traditional Chinese Medicine, Lu'an, China*

Correspondence should be addressed to Jun Dai; wxxydaijun@163.com and Bangxing Han; hanbx1978@sina.com

Received 10 September 2023; Revised 24 November 2023; Accepted 27 December 2023; Published 5 February 2024

Academic Editor: Akhilesh K. Verma

Lipid metabolism disorders are widely acknowledged as crucial risk factors for a range of metabolic diseases, including hyperlipidemia, obesity, nonalcoholic fatty liver disease, and atherosclerosis. Dysbiosis of the gut microbiota is considered a potential mechanism of action in lipid metabolism disorders. *Dendrobium huoshanense* C.Z. Tang et S.J. Cheng (DH), an important edible and medicinal Chinese herb, has been shown to regulate the gut flora disorders and improve intestinal health. However, DH inhibits lipid metabolism disorders by regulating the gut flora remains unclear. Therefore, we aimed to explore the effect of the gut flora on improving blood lipid levels in mice that fed a high-fat diet supplemented with DH. Mice were randomly divided into normal control (CTR), high-fat diet (HFD), 2.25 mg/kg/day simvastatin (SIM), 300 mg/kg/day DH (LD-DH), and 600 mg/kg/day DH (HD-DH) groups for 14 weeks. Changes in serum and liver lipid levels and liver function were analyzed. Changes in intestinal microbiota and fecal metabolites were assessed using 16S rRNA gene sequencing and untargeted metabolomics. The relationships among lipids, intestinal microbiota, and fecal metabolites were analyzed using Pearson's correlation analysis to reveal the mechanism of action of DH against lipid metabolism disorders. The results indicated that DH effectively improved the lipid profiles in both the serum and liver of HFD mice. DH was also found to alter the structure of the gut flora, especially the relative abundances of *Bifidobacterium pseudolongum* and *B. animalis*, which dramatically increased with DH. Pearson's correlation analysis indicated that DH may mainly alter metabolites (amino acid metabolites, bile acid metabolites, lipid metabolites, etc.) to regulate lipid metabolism via the metabolic ability of the gut flora. *B. pseudolongum* and *B. animalis* may be the dominant bacterial species in the gut microbiota and play key roles in the alleviation of lipid metabolism disorders caused by HFD.

1. Introduction

With changes in lifestyle and aging, lipid metabolism disorders (LMDs) were becoming increasingly prevalent annually. LMD was a major risk factor for metabolic diseases, such as hyperlipidemia, obesity, and atherosclerosis [1] and seriously threatened human health. Therefore, it was crucial to seek effective therapeutic targets to prevent and treat LMD to promote and improve quality of life.

The gut microbiota was commonly known as an important "metabolic organ," which consisted trillions of microorganisms in the human and animal guts and had a very strong metabolic ability. In recent years, numerous studies had shown that homeostatic gut flora contributed to normal host metabolism. However, disorders in the structure and function of the gut flora, which was induced by HFD [2, 3], could promote the onset and progression of LMD [4, 5]. Studies had shown that the proportion of beneficial gut flora, such as *Bifidobacteria* and *Lactobacillus*, was markedly reduced in hyperlipidemic mice fed a HFD, and the loss of these bacteria was strongly correlated with higher lipid levels [6]. *Bifidobacterium* species alleviated

LMD and intestinal flora dysbiosis [7]. *B. pseudolongum* had been shown to interact with jackfruit seed-derived resistant starch, significantly reducing serum lipid levels and hepatic damage in mice [8]. *B. pseudolongum* treatment significantly ameliorated intestinal flora dysbiosis and reduced plasma triacylglycerol (TG) levels, as well as reducing body mass and visceral fat [9]. *B. animalis* subsp. A6 had been shown to inhibit the development of obesity by increasing fatty acid oxidation in adipose tissue [10]. In addition, *B. pseudolongum*, *B. animalis*, and *Lactobacillus salivarius* could promote the fecal excretion of bile acids and regulate bile acid-mediated lipid metabolism by producing bile salt hydrolase (BSH), which hydrolyzed conjugated bile acids into free bile acids that were difficult to reabsorb in the intestinal tract [11–13].

DH was harvested from the Da-bie Mountains of China, with a high concentration of plants found in Huoshan County, Anhui Province, China. The plant, known locally as "Mihu," was registered in the 2020 edition of "Pharmacopeia of the People's Republic of China" (the *Pharmacopeia*) and approved for use as a food material [14]. The main active substances in DH included flavonoids, alkaloids, and polysaccharides, which played important therapeutic roles and polysaccharides was an index of the quality control of DH in the *Pharmacopeia* [14]. DH benefited the stomach, promoted fluid production, nourished yin, and promoted clearance [14]. Modern pharmacological studies had confirmed that DH had various activities, such as immunoregulation [15], gastric mucosal protection [16], and protection against liver injury [17], which aided in preventing and curing diseases, strengthening the body, and prolonging life. DH polysaccharides had been shown to decrease the levels of total cholesterol (TC), TG, and malondialdehyde and protect against high-cholesterol diet-induced atherosclerosis [18]. DH treatment also alleviated ethanol-induced liver injury in HFD mice by restoring perturbed metabolic pathways [19]. DH polysaccharides could improve the composition of the gut flora, promoted the proliferation of *Lactobacillus* and *Owenweeksia*, and enhanced the function of the intestinal barrier by upregulating the expression of tight junction proteins, mucin-2, beta-defensins, and cytokines [20]. After 18 weeks, DH significantly lowered serum TG levels and inhibited the progression of atherosclerosis induced by a HFD in $LDLR^{-/-}$ mice [21]. In hyperlipidemic rats, the administration of DH also resulted in a significant reduction in serum TG levels, as well as TC, and low-density lipoprotein cholesterol (LDL-C) levels and increased high-density lipoprotein cholesterol (HDL-C) levels [22]. Although previous studies had shown that the administration of DH had beneficial effects on lipid metabolism and intestinal flora, the mechanism of action of DH in the relationship between lipid metabolism and changes in the intestinal flora remained unclear.

In this study, we evaluated the effects of DH on LMD amelioration in HFD mice. Furthermore, we analyzed whether DH could modulate the structure of the gut flora and its fecal metabolites, as well as their relationship with lipid metabolism to provide theoretical evidence for the development of DH to prevent LMD.

2. Materials and Methods

2.1. Materials. DH extract was supplied by Jiuxianzun Huoshan Dendrobium Co., Ltd., and all ELISA/biochemical kits used in the experiments were purchased from Multi-sciences Biotech Co., Ltd./Nanjing Jiancheng Bioengineering Institute.

2.2. HPLC-MS/MS Analysis of DH. The ingredients of the DH extract were analyzed using a high-performance liquid chromatography tandem mass spectrometry (LC-MS/MS). Samples for LC-MS/MS detection were prepared as previously described [23]. LC-MS/MS analyses were performed as previously reported [24, 25].

2.3. Establishment of the LMD Model and Treatments. Thirty-five male six-week-old mice (weighing 20 ± 2 g) were purchased from Gempharmatech Co., Ltd. (Jiangsu, China). The mice were housed in the laboratory under the following conditions: temperature: $25 \pm 1^{\circ}C$; relative humidity: $55 \pm 10\%$; and 12 h dark: 12 h light. The mice were fed a standard diet for one week and had free access to drinking water. One week later, the mice were randomized into five treatment groups ($n = 7$) and fed different diets. The control group (CTR) was received normal chow diet (NCD; XT93; 10% calories from fat) with free access to water. The model group (HFD) was fed a high-fat diet (HFD; XTHF60; 60% calories from fat), with free access to water. The positive control group (SIM) was fed the HFD plus daily administration (by gavage) of 2.25 mg/kg/day simvastatin, according to previous studies [26, 27]. The low-dose DH group was administered HFD plus a daily administration of 300 mg/kg/day DH (daily LD-DH), and the high-dose DH group was fed the HFD plus daily administration of DH by gavage of 600 mg/kg/day (HD-DH), according to previous studies [28, 29]. All animals were fed for 14 weeks. Normal chow diet and high-fat diet were purchased from Xietong Pharmaceutical Bio-engineering Co., Ltd. (Jiangsu, China).

2.4. Collection of Feces and Tissue Samples. At the end of the experiment, all mice were starved for 12 h, during which time only water was provided. Fresh fecal samples were obtained from each mouse for gut flora and fecal metabolomic analyses, and all mice were anesthetized and sacrificed. Blood samples were obtained from the orbit, maintained for 30 min at $25 \pm 1^{\circ}C$ before centrifugation (6,000g for 10 min) at 4°C to obtain the blood serum, and stored in a refrigerator at −80°C. The livers were removed from each of the sacrificed mice and cleaned with phosphate-buffered saline (PBS). Then, one part was stored in the refrigerator at −80°C and the other parts were stored in 4% polyformaldehyde for further analysis.

2.5. Biochemical Analysis. The serum TC, TG, alanine aminotransferase (ALT), and aspartate aminotransferase (AST) levels were analyzed using commercially available kits. The first part of the collected liver tissue sample stored

at −80°C was cleaned with deionized water, and liver tissue (0.5 g) from each mouse was ground with physiological saline using a homogenizer to prepare the liver homogenate, which was then centrifuged (2,000*g* for 10 min) to obtain the supernatant. The levels of TC, TG, ALT, and AST in the liver were analyzed using commercially available biochemical kits. All analyses were performed according to the manufacturer's instructions.

2.6. Oil Red and HE Staining of Liver. Next, hepatic histopathologic examinations were conducted by oil red O and HE staining of liver. Oil red O and HE staining of liver was performed as previously described method [30]. Image-Pro Plus 6.0 software was used for quantitative analysis.

2.7. Analysis of Intestinal Microflora. The fresh fecal samples that had been collected from each mouse before sacrifice were prepared for 16S rRNA sequencing. Briefly, the V3 and V4 hypervariable regions of the 16S rRNA were amplified (forward primer: ACTCCTACGGGAGGCAGCA; reverse primer: GGACTACHVGGGTWTCTAAT), and amplification and quality control of the raw data were performed on the Illumina platform. Sequence denoising or clustering was performed using the DADA2 method, in which data were only deduplicated or clustered based on 100% similarity. Taxonomic composition analysis was performed and visualized using QIIME2. PCoA and NMDS analyses were performed and visualized using the R software. Raw sequencing data were saved in the FASTQ format.

2.8. Metabolic Analysis. Fecal samples, each weighing 100 mg, were placed in 2-mL grinding tubes, each containing 50 mg of zirconia beads. Next, 200 mL of ultrapure water was placed into the grinding tube and homogenized in a grinder (Servicebio KZIII-F) at the maximum speed for 30 s to obtain the fecal homogenate. Then, 400 μL of methanol : acetonitrile (volumetric ratio of 1 : 1) was added to the homogenized samples. The solution was vortexed for 30 s, followed by extraction for 30 min in an ultrasonic extractor (KQ-600DE; Kunshan Ultrasonic Instruments Co. Ltd., Kunshan, China) at a low temperature. After the homogenized samples were centrifuged at 13,500*g* for 20 min, the supernatants were transferred to EP tubes and dried using a nitrogen blower. Finally, the residue was reconstituted with 200 μL of methanol : acetonitrile (1 : 1) and centrifuged at 13,500*g* for 20. Lastly, a 3-μL aliquot was injected into the UPLC–QTOF/MS (Thermo Q Exactive Orbitrap) for analysis [25].

2.9. Statistical Analysis. Differences between two or more groups were assessed using Student's *t*-test and one-way analysis of variance (ANOVA), respectively. Data were presented as the mean ± standard deviation (SD). Statistical analyses were performed using SPSS version 22.0. The figures were processed using GraphPad Prism software (version 9.0). Except for special instructions, $p < 0.05$ and $p < 0.01$ were considered statistically significant. Correlations between the gut flora, fecal metabolites, and lipid metabolic indicators were assessed using Pearson's correlation analysis.

3. Results

3.1. Qualitative Analysis of DH. The content of polysaccharides in the DH extract was 426.84 mg/g, which was measured by the phenol-sulfuric acid method, according to "Pharmacopeia of the People's Republic of China" (2020). The chemical ingredients of the DH extract were analyzed using LC-MS. Hundreds of chemical ingredients were found in the DH extract according to positive and negative ion modes, most of which exhibited sharp symmetrical peaks, indicating good separation. Twenty-one major ingredients were identified in the DH extract according to the major fragments in the MS spectra, as shown in Table 1.

3.2. DH Administration Improved Dyslipidemia in HFD Mice. Changes in the body weight and serum lipid levels were measured after 14 weeks of feeding (Figure 1). Compared to the CTR group, the body weight and TG and TC levels in the serum of the HFD group were markedly increased, indicating that the hyperlipidemic mouse model was successfully induced by HFD. At the same time, mice treated with different doses of DH or SIM exhibited lower body weights and TG and TC levels than HFD mice, indicating that DH effectively improved dyslipidemia in HFD mice.

3.3. DH Administration Ameliorated Liver Function Damage in HFD Mice. Liver function disorders were analyzed in the five groups of mice. Increased hepatic steatosis and lipid deposition in the liver were observed in the HFD group than the CTR group (Figures 2(a)–2(d)). In contrast, DH treatment significantly decreased hepatic steatosis and lipid deposition (Figures 2(a)–2(d)). In addition, the liver index of the HFD mice was significantly increased compared to the CTR group, while the liver index of mice treated with DH was significantly decreased (Figure 2(e)). Compared to the CTR group, the HFD group had higher levels of serum AST and ALT, hepatic TC, TG, AST, and ALT, which were reversed by DH (Figures 2(f)–2(k)). These results suggested that DH improved liver function damage induced by HFD. A regulatory effect on liver function was also exhibited in SIM-treated mice.

3.4. DH Treatment Reversed Gut Microbial Dysbiosis in HFD Mice. To study the effects on intestinal flora in HFD-induced hyperlipidemia mice given DH, 16S rRNA sequencing on mouse feces was performed. There was no significant difference in species richness of gut microbiota among different groups of mice (Figure 3(a)). At the phylum level, the relative abundances of *Actinobacteria*, *Proteobacteria*, *TM7*, *Tenericutes,* and *Fusobacteria* of HFD mice were decreased with DH treatment (Figure 3(b)). In addition, the relative abundances of bacterial species at the genus and species levels in different treatment groups were

Table 1: Ingredients identified in the DH extract.

Compounds	Formula	Reference ion	T (min)	MZ	Pos/Neg
L-malic acid	$C_4H_6O_5$	$[M-H]^-$	0.747	133.014	Neg
Adenosine	$C_{10}H_{13}N_5O_4$	$[M+H]^+$	1.225	268.105	Pos
Catechol	$C_6H_6O_2$	$[M]^+$	9.787	110.019	Pos
D-Mannose	$C_6H_{12}O_6$	$[M-H]^-$	1.238	179.056	Neg
Shikimic acid	$C_7H_{10}O_5$	$[M-H]^-$	0.79	173.045	Neg
Apigenin	$C_{15}H_{10}O_5$	$[M-H]^-$	7.39	269.046	Neg
Resveratrol	$C_{14}H_{12}O_3$	$[M-H]^-$	5.47	227.071	Neg
Uridine	$C_9H_{12}N_2O_6$	$[M-H]^-$	1.225	243.062	Neg
Naringenin	$C_{15}H_{12}O_5$	$[M+H]^+$	6.19	273.075	Pos
(+)-Syringaresinol O-beta-D-glucoside	$C_{28}H_{36}O_{13}$	$[M-H]^-$	4.938	579.191	Neg
Gardenoside	$C_{17}H_{24}O_{11}$	$[M\text{-}H_2O\text{-}H]^-$	4.397	385.115	Neg
(+)-Syringaresinol	$C_{22}H_{26}O_8$	$[M-H]^-$	4.935	417.154	Neg
Quercetin	$C_{15}H_{10}O_7$	$[M-H]^-$	10.702	301.237	Neg
Rutin	$C_{27}H_{30}O_{16}$	$[M]^+$	11.448	610.16	Pos
Syringic acid	$C_9H_{10}O_5$	$[M+H]^+$	2.218	199.06	Pos
Coniferyl aldehyde	$C_{10}H_{10}O_3$	$[M+H]^+$	1.943	179.07	Pos
4-Hydroxybenzaldehyde	$C_7H_6O_2$	$[M+H]^+$	1.23	123.044	Pos
p-Coumaroyl-D-glucose	$C_{15}H_{18}O_8$	$[M-H]^-$	1.45	325.093	Neg
D-glucopyranoside	$C_6H_{12}O_6$	$[M\text{-}H_2O\text{-}H]^-$	10.078	161.048	Neg
Taxifolin	$C_{15}H_{12}O_7$	$[M\text{-}H_2O\text{-}H]^-$	5.728	285.04	Neg
Isoeugenol	$C_{10}H_{12}O_2$	$[M+H]^+$	4.85	165.092	Pos

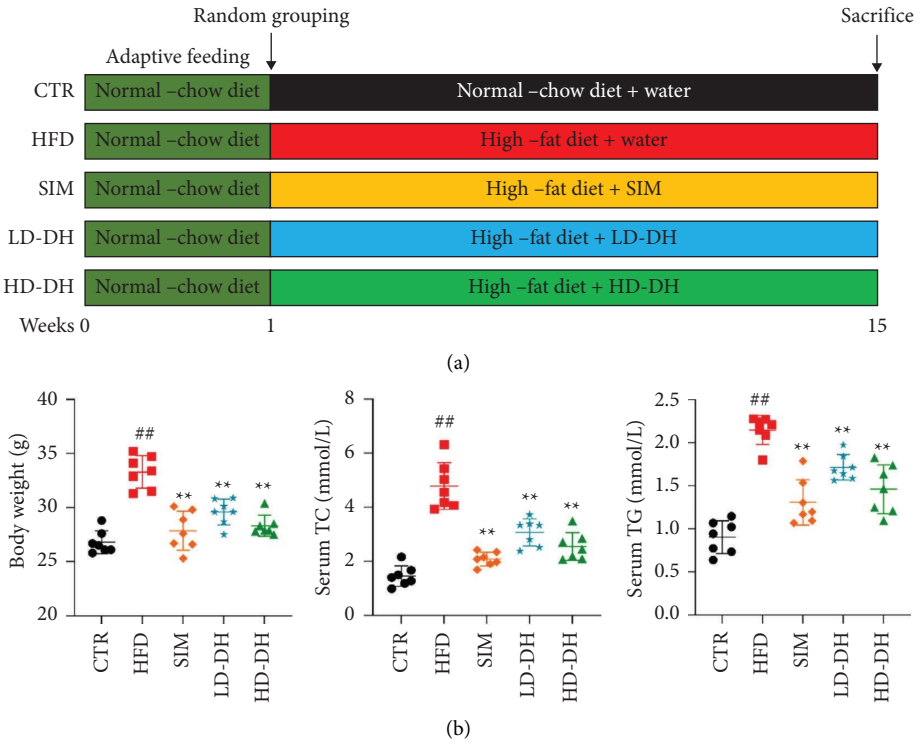

Figure 1: Administration of DH improved dyslipidemia in mice fed HFD. (a) Schematic diagram of DH treatment. (b) Body weight of mice at the end of experiment, and the levels of TG and TC in serum were tested using commercial biochemical kits. $^{\#\#}p < 0.01$and $^{**}p < 0.01$ vs. HFD or CTR groups.

compared. The abundances of *Allobaculum* and *Rikenella* in the HFD group were markedly lower than the corresponding values in the CTR group. In contrast, *Clostridiaceae clostridium*, *Helicobacter,* and *Odoribacter* were more abundant in the HFD group. In the HD-DH treatment group, the abundances of *Allobaculum* and *Bifidobacterium* were markedly higher than those in the HFD group, whereas the abundances of *Clostridiaceae clostridium* and *Streptococcus* were lower (Figures 3(c) and 3(e)). At the species level, the abundances of *Clostridium celatum* and *Lactobacillus*

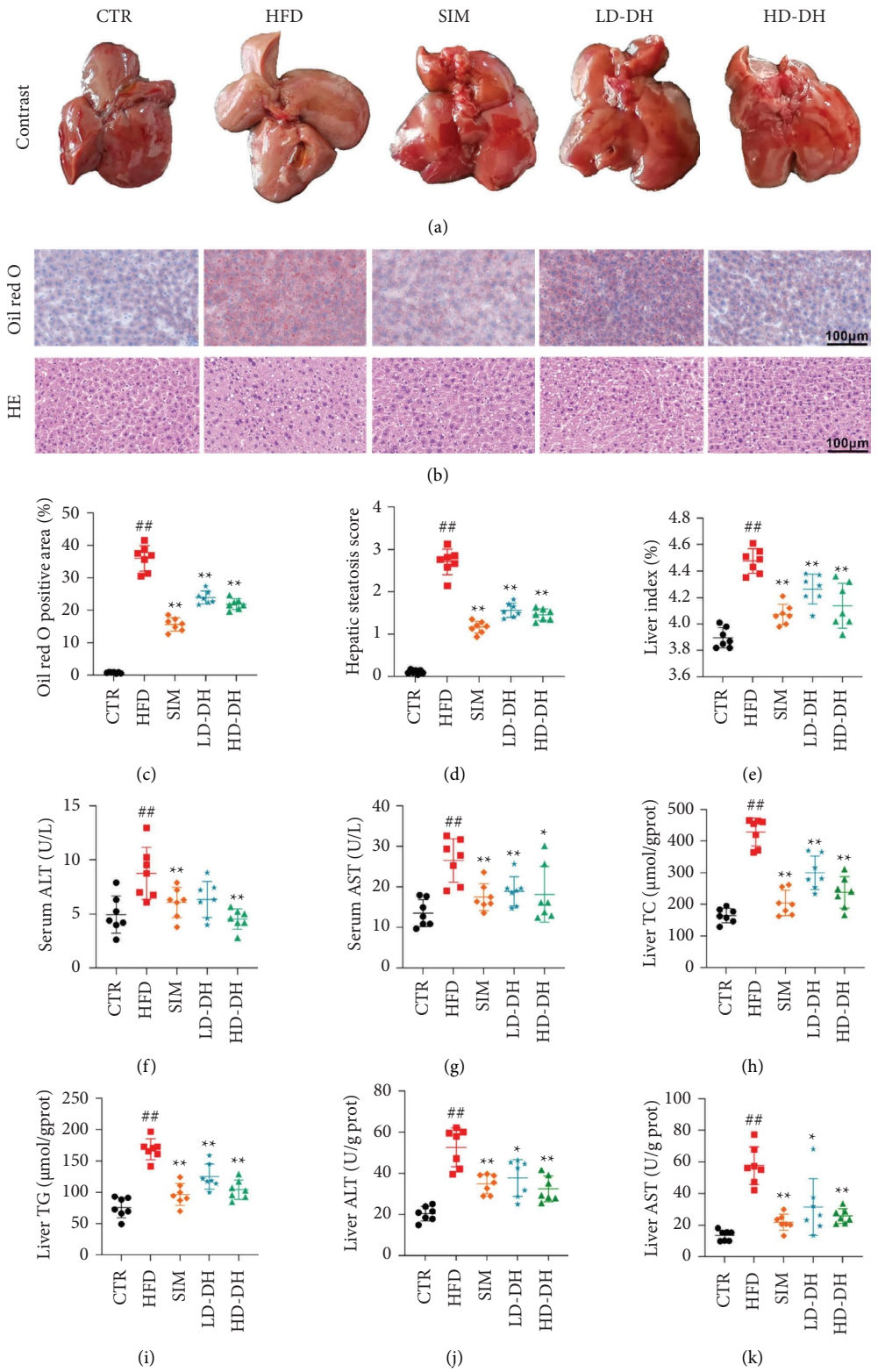

FIGURE 2: DH treatment ameliorated liver function damage in HFD mice. (a) Mouse liver photographs in each experimental group. (b) Oil red O and HE staining images of mice liver tissue. (c) Oil red O positive area (%). (d) Hepatic steatosis score. (e) Changes in the liver index (liver weight/body weight). The levels of ALT (f) and AST (g) in serum, and the levels of TC (h), TG (i), ALT (j), and AST (k) in mice liver were measured using commercial biochemical kits. $^{\#\#}p < 0.01$, $^{*}p < 0.05$, and $^{**}p < 0.01$ vs. HFD or CTR group.

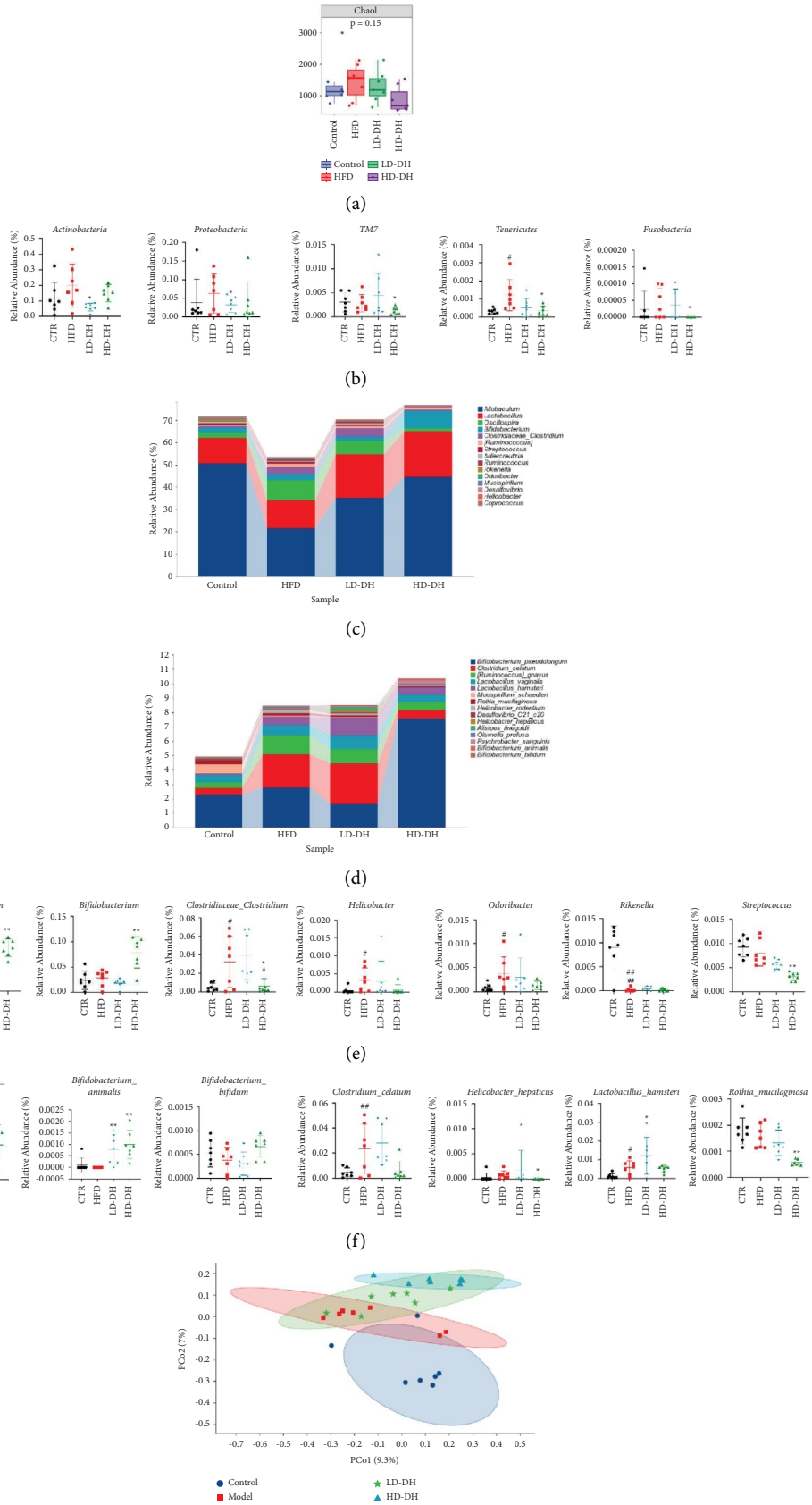

Figure 3: Continued.

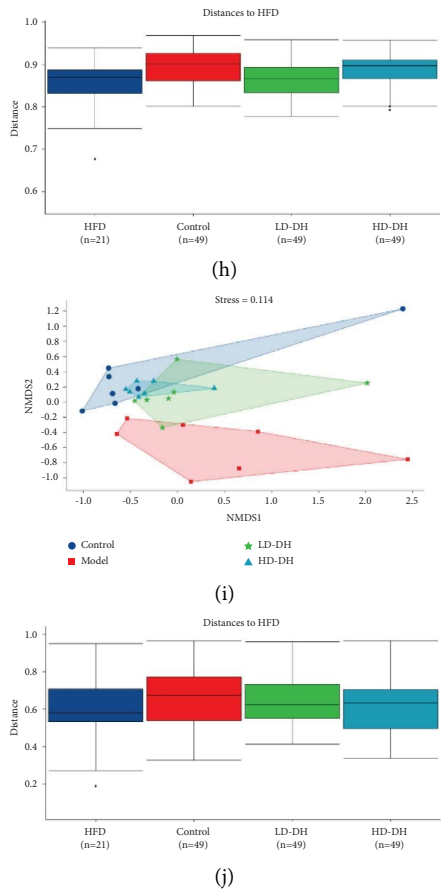

Figure 3: Effects of DH on intestinal flora in HFD mice. (a) The chao1 index for alpha diversity analysis. (b) Relative abundance of differential specific taxa at the phylum level. (c) Intestinal flora composition profile at the genus level. (d) Intestinal flora composition profile at the species level. (e) Relative abundance of specific taxa at the genus level. (f) Relative abundance of specific taxa at the species level. (g) PCoA and (i) NMDS analysis for beta diversity analysis. (h) Adonis analysis for intergroup differences. (j) Anosim analysis for intergroup differences.

hamsteri were markedly higher in the HFD group than in the CTR group. In contrast, compared to the HFD group, *B. pseudolongum* and *B. animalis* were markedly higher in the HD-DH group, whereas the abundances of *Helicobacter hepaticus* and *Rothia mucilaginosa* were lower (Figures 3(d) and 3(f)).

Furthermore, a significant difference in the gut microbiota structure in mice was observed by beta diversity analysis based on PCoA and NMDS analysis and intergroup differences between the HFD and CTR, HFD, and treatment groups (Figures 3(g)–3(j)). The results indicated that the gut flora structure in the HFD group was significantly different from that in the CTR group. However, the community structure in the HD-DH group was markedly different from that in the HFD group, indicating that DH altered the gut microbiota structure in the HFD group.

In order to explore the metabolic regulation function of gut microbiota, PICRUSt2 software was used to predict the function of gut microbiota (Figure 4). Based on the comparison of the KEGG database, it was found that the main first-level classification of functional pathways including 6 categories, namely, metabolism, genetic information processing, environmental information processing, cellular processes, organismal systems, and human diseases. Among them, there were 28 metabolic pathways in the KEGG secondary-level classification of functional pathways, with higher abundance concentrated in metabolism, mainly including amino acid metabolism, lipid metabolism, carbohydrate metabolism, and metabolism of terpenoids and polyketides. Among them, the relative abundance of lipid metabolism in HD-DH was increased than in the HFD group, while amino acid metabolism in HD-DH was decreased than in the HFD group.

3.5. DH Significantly Altered the Profile of Fecal Metabolites from Intestinal Microbiota in HFD Mice. Gut metabolites affected by the intestinal microbiota may alter host metabolism. Differential fecal metabolites in mice were evaluated using nontargeted metabolic profile analysis (Figure 5). Score plots of PLS (Figures 5(a)–5(c)), OPLS (Figures 5(b)–5(d)), and PCA (Figures 5(i)–5(j)) (positive and negative) showed that the CTR, HFD, and HD-DH groups were significantly different from each other, suggesting that the levels of gut metabolites in the CTR group were changed markedly by a HFD, and that this elevation in metabolites could be reversed by DH.

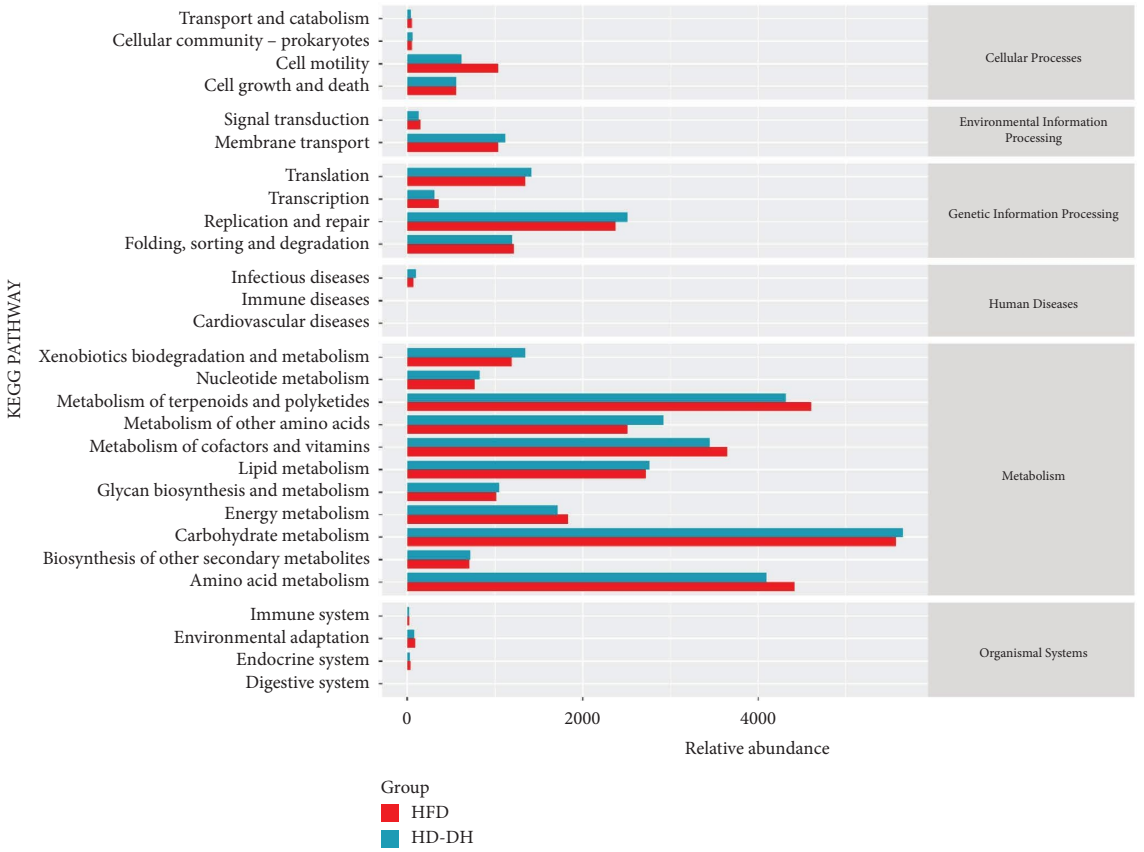

Figure 4: Metabolic pathway statistics.

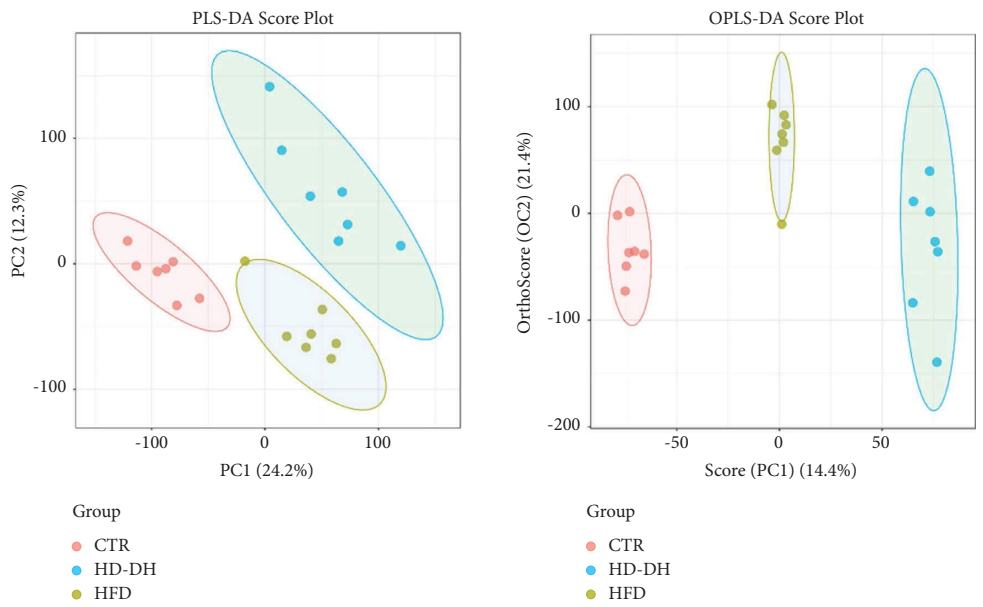

Figure 5: Continued.

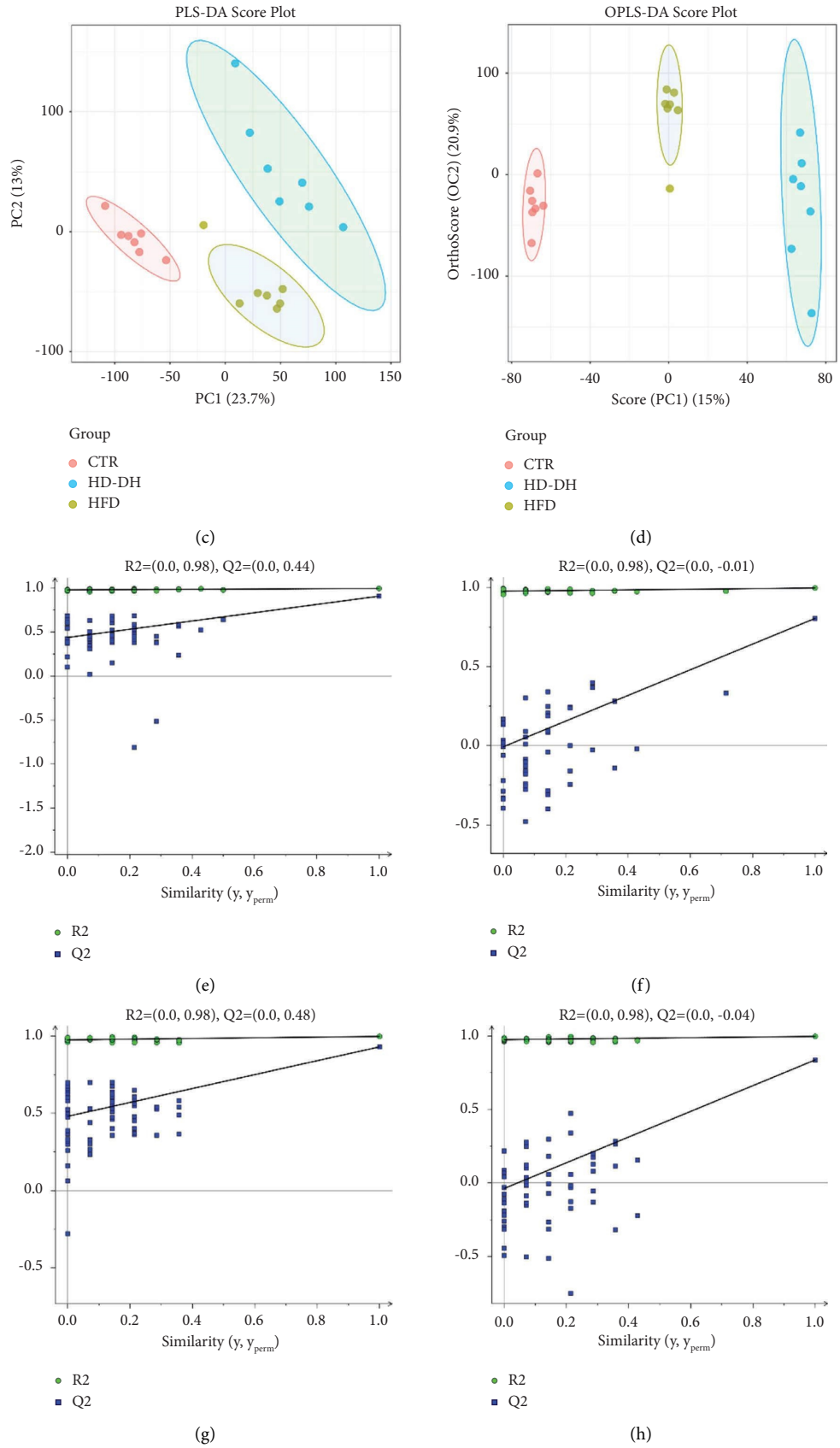

Figure 5: Continued.

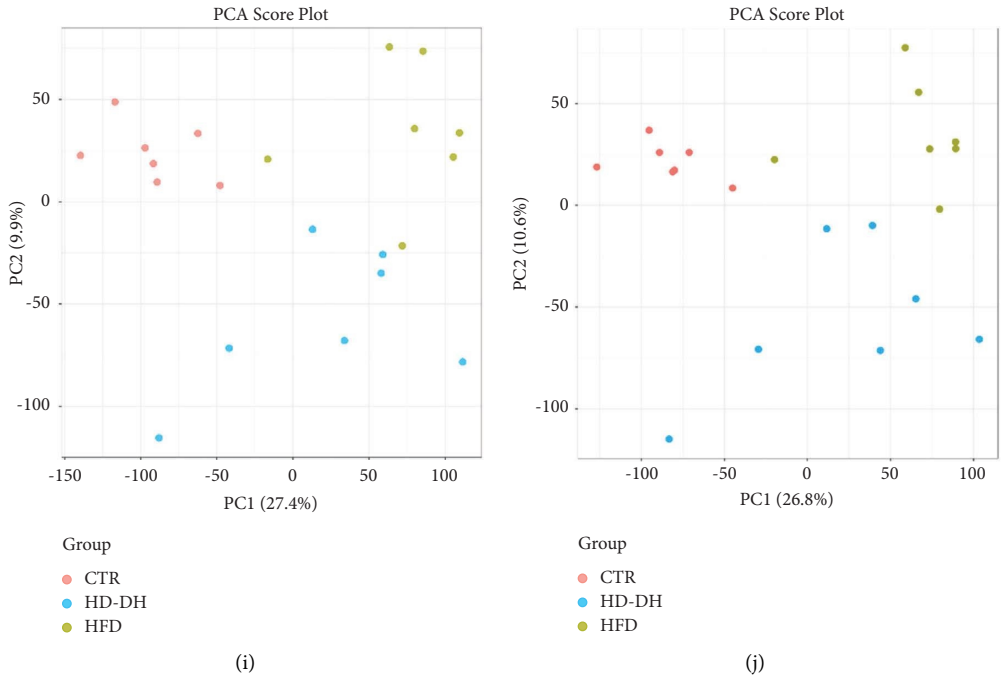

Figure 5: The profile of fecal metabolites from gut microbiota in HFD mice was markedly changed by DH. (a) Positive PLS-DA score plot. (b) Positive OPLS-DA plot. (c) Negative PLS-DA score plot. (d) Negative OPLS-DA plot. (e) The permutation test following PLS-DA model in positive mode. (f) The permutation test following OPLS-DA model in positive mode. (g) The permutation test following PLS-DA model in negative mode. (h) The permutation test following OPLS-DA model in negative mode. (i) Positive PCA score plot. (j) Negative PCA score plot.

A total of 60 critical metabolites from feces showed significant changes among the three groups based on the threshold of VIP (>1.5) and p (<0.05) between the HFD and HD-DH groups (Figure 6(a)). Among these, 17 metabolites were significantly increased and two metabolites were markedly decreased in the HFD group than the results from the CTR group, which were all reversed by DH (Figure 6(b)), which is closely related to lipid metabolism. These metabolites were found to be mainly associated with bile secretion (deoxycholic acid and acetylcholine), steroid hormone biosynthesis (cholesterol sulfate), fatty acid biosynthesis (stearic acid), urine and nucleotide metabolism ((S)-ureidoglycine, guanosine, and xanthosine), arginine and proline metabolism (agmatine, D-ornithine, citrulline, guanidoacetic acid, and cis-4-hydroxy-D-proline), lysine degradation (5-aminopentanoic acid and glutaric acid), aminoacyl-tRNA biosynthesis (L-methionine and L-valine), glutathione metabolism (gamma-glutamylalanine), and arachidonic acid metabolism (20-HETE) (Figure 7). In conclusion, bile acid, lipid, and amino acid metabolism in the HFD group were altered by DH.

3.6. Mechanism of DH against Dyslipidemia Revealed by Pearson's Correlation Analysis. Pearson's rank correlation analysis was used to analyze the correlations among the 22 altered fecal metabolites, biochemical parameters, and gut microbiota in the HFD and HD-DH groups. The altered gut microbiota and biochemical parameters of species, such as *B. pseudolongum* and *B. animalis*, showed significant negative correlation with the TG, TC, ALT, and AST levels in the serum and liver. *Desulfovibrio_C21_c20* and *B. bifidum* were significantly negatively correlated with the TC levels (Figure 8(a)). In addition, *Rothia mucilaginosa*, *Helicobacter hepaticus,* and *Clostridium celatum* were significantly positively correlated with the TG, TC, ALT, and AST levels in the serum or liver. These results suggest that the aforementioned intestinal bacteria, such as *B. pseudolongum* and *B. animalis,* may be critical for the beneficial effects of DH. Next, the correlations between the 22 altered metabolites and biochemical parameters were evaluated (Figure 8(b)). The results showed that the metabolites stearic acid, xanthosine, deoxycholic acid, 20-HETE, and cholesterol sulfate were negatively correlated with these biochemical parameters. The fecal metabolites except for the abovementioned 5 metabolites showed significantly positive correlation with these biochemical parameters. Correlations between gut flora species and fecal metabolites were also observed (Figure 8(c)). The results showed that xanthosine was markedly positively correlated with *B. pseudolongum*, whereas stearic acid, deoxycholic acid, and cholesterol sulfate were significantly positively correlated with *B. animalis*. *B. pseudolongum* and *B. animalis* were markedly negatively correlated with cis-4-hydroxy-D-proline, gamma-glutamylalanine, N-acetyl-L-glutamine, L-methionine, guanidoacetic acid, (S)-ureidoglycine, acetylcholine, 2-methylserine, agmatine, 5-hydroxypentanoic acid, L-valine, L-prolinamide, or citrilline. However, *Rothia mucilaginosa or Clostridium celatum* showed significant positive correlation with metabolites, such as L-methionine, guanidoacetic acid, D-ornithine, (S)-ureidoglycine, glycylleucine,

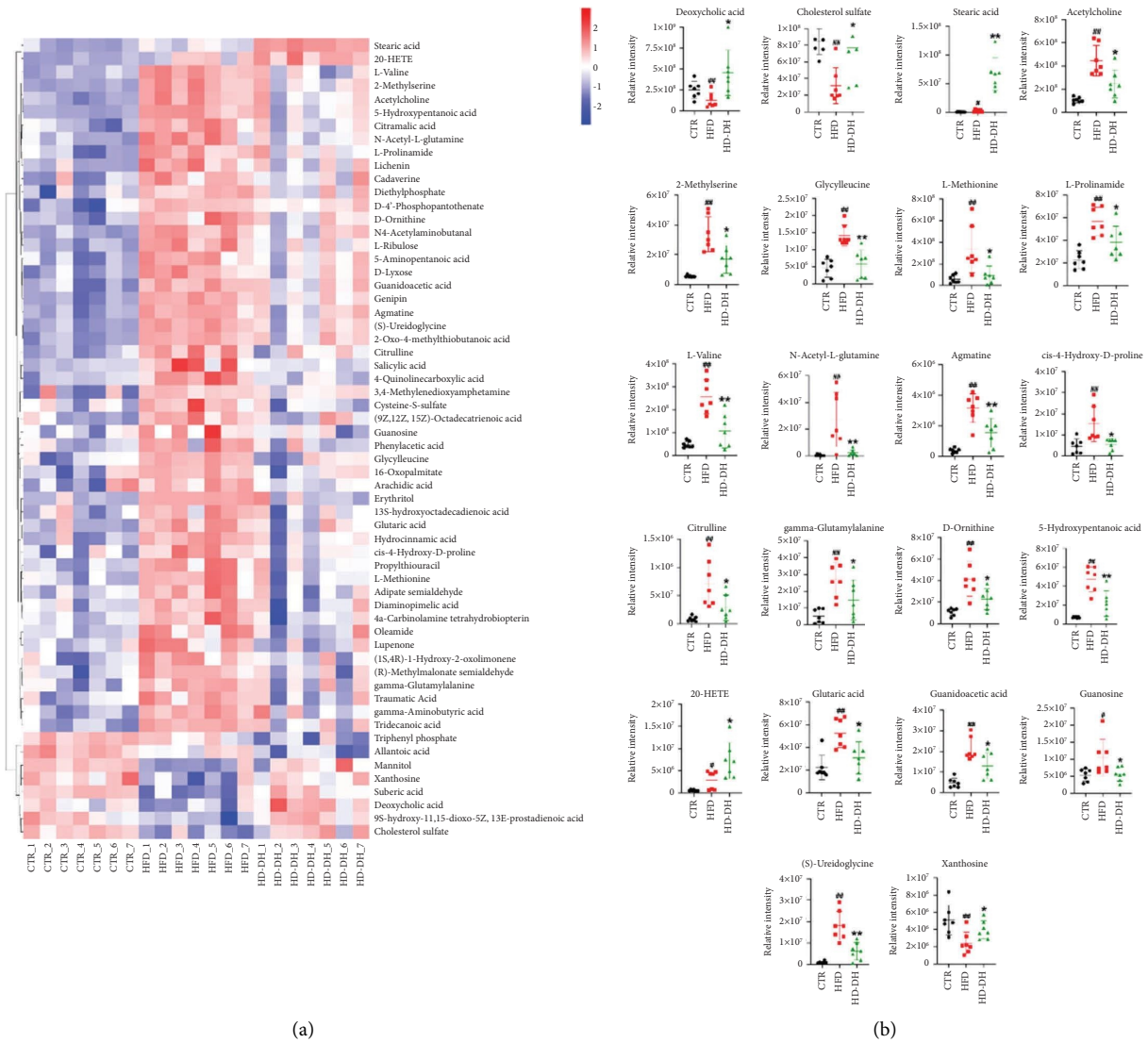

(a) (b)

Figure 6: Relative contents of critical biomarkers in the CTR, HFD, and HD-DH groups. (a) Heatmap analysis of potential biomarkers. (b) The results of 22 differential fecal metabolites among the CTR, HFD, and HD-DH groups. $^{\#}p < 0.05$, $^{\#\#}p < 0.01$, $^{*}p < 0.05$, and $^{**}p < 0.01$ vs. HFD or CTR group.

acetylcholine, 2-methylserine, 5-hydroxypentanoic acid, L-valine, L-prolinamide, or citrilline, and negative correlation with stearic acid, 20-HETE, xanthosine, or cholesterol sulfate. These results show that DH plays an antihyperlipidemic role by regulating fecal metabolites via probiotics *B. pseudolongum* and *B. animalis*.

4. Discussion

In this study, not only were the levels of TC, TG, AST, and ALT reduced in the serum and liver, but the hepatic steatosis and lipid accumulation were increased in the liver of the HFD group, which was reversed by DH. These findings suggested that DH could inhibit lipid disorders and restore liver function in the HFD group.

To elucidate the modulatory mechanism of DH in LMD, the structure of the mouse gut microbiota was explored using high-throughput 16S rRNA gene sequencing. Interestingly, different doses of DH significantly altered the structure of the intestinal flora and inhibited the structural dysbiosis of the gut flora in the HFD group. Furthermore, HD-DH upregulated the relative abundance of *Allobaculum* and *Bifidobacterium* at the genus level and *B. pseudolongum* and *B. animalis* at the species level.

B. animalis subsp. *lactis* BB-12 inhibited obesity by regulating intestinal flora in two phases in human flora-associated rats [31]. In overweight and obese children, the body mass index and serum levels of TC and LDL-C were reported to decrease significantly after 12 weeks of treatment with supplementary probiotics, including *B. animalis* CP-9 in a double-blind, randomized, placebo-controlled trial [32]. *B. animalis* attenuated the inflammatory response and reduced lipid accumulation in mice with nonalcoholic fatty liver disease (NAFLD)

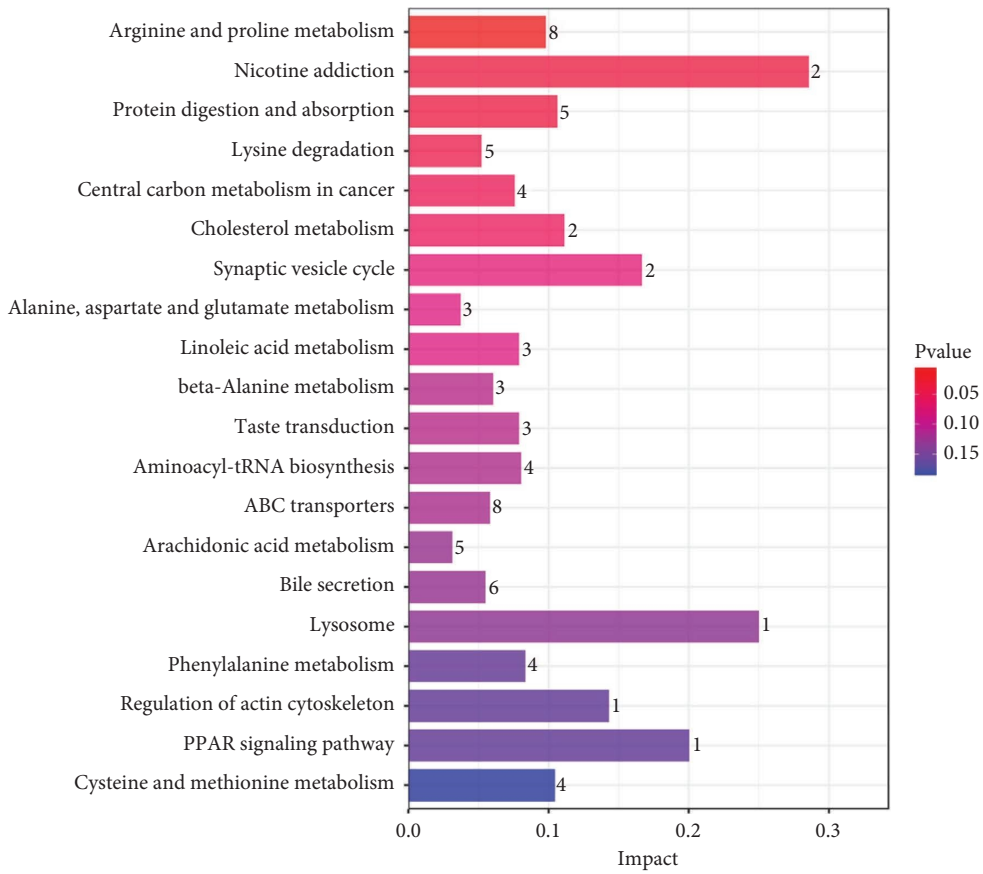

Figure 7: Statistics on the number of differentially expressed molecules in the KEGG pathway.

[33]. Oligofructose supplementation rapidly increased the relative abundance of *B. pseudolongum,* which mediated gut lipid-sensing mechanisms to reduce food intake and obesity [34]. Those results were consistent with our study that DH promoted proliferation of *B. pseudolongum* and reduce obesity, liver index, and lipid levels of hyperlipidemic mice.

The relative abundances of *B. pseudolongum* and *B. animalis* enriched by DH were negatively correlated with biochemical parameters, such as lipid levels and liver injury markers, and *Helicobacter hepaticus*, *Rothia mucilaginosa,* and *Clostridium celatum* inhibited by DH were positively correlated these biochemical parameters. These results suggested that an increase in the regulating-lipid microbial species of *B. animalis* and *B. pseudolongum* was the main mechanism by which DH alleviated lipid metabolism disorders.

To further explore the mechanism of DH in LMD, the metabolite profiles of the intestinal microbiota were analyzed using fecal metabolomics. The results showed that DH could alter the fecal metabolite profiles of HFD mice.

Especially, DH significantly promoted excretion of fecal deoxycholic acid, stearic acid, and cholesterol sulfate. The excretion levels of fecal metabolites, such as deoxycholic acid, xanthosine, and cholesterol sulfate promoted by DH, were negatively correlated with biochemical parameters. Desoxycholic acid, a secondary bile acid, was converted from primary intestinal bile acids by gut bacteria, such as *Bifidobacterium* spp. *Bifidobacterium* could lead to higher levels of deoxycholic acid [35]. Evidence indicated that secondary bile acids, such as deoxycholic acid and lithocholic acid, were toxic bile acids associated with LMD and gastrointestinal diseases [36]. Increasement of fecal excretion of deoxycholic acid, stearic acid, and cholesterol sulfate, could reduce hepatic cholesterol and decrease lipogenesis. *B. animalis* subsp. *lactis* F1-7 reduced the TG, TC, LDL-C, and HDL-C levels in the serum, and the TC and TG levels in the liver of HFD mice, while total bile acids were increased in feces, which improved hyperlipidemia in HFD mice by downregulating FXR [37]. Those results were consistent with our research that DH promoted proliferation of *B. animalis* and the excretion of fecal bile acid and improved lipid metabolism.

In addition, most amino acid metabolic pathways were enriched in HFD mice and DH supplementation suppressed the metabolic levels of these amino acids in the gut microbiota, which was consistent with the previous research [38]. The metabolite levels of amino acid metabolism (such as L-valine, cis-4-hydroxy-D-proline, and gamma-glutamylalanine) inhibited by DH positively correlated these biochemical parameters. Evidence suggested branched-chain amino acids including L-valine could cause insulin resistance and glucose metabolism disorder [39]. HFD could induce disorders of lipid metabolism and amino acid metabolism. *Sporisorium reilianum* polysaccharide

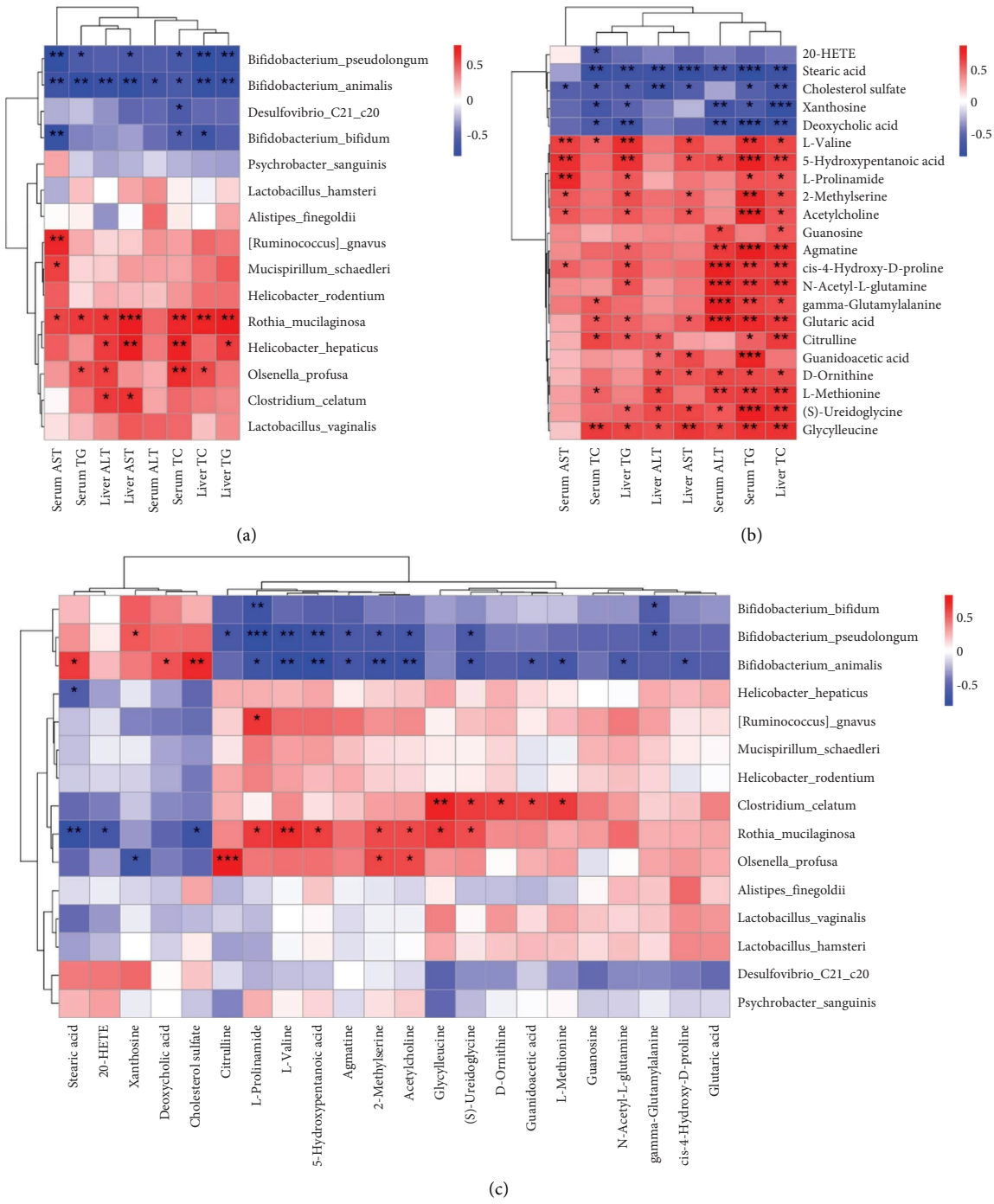

FIGURE 8: The results of Pearson's correlation analysis of omics data displayed as heatmaps. (a) Biochemical parameters and microbial species abundances. (b) Biochemical parameters and fecal metabolites. (c) Microbial species abundances and fecal metabolites. $^{*}p < 0.05$, $^{**}p < 0.01$, and $^{***}p < 0.001$.

significantly alleviated obesity via gut microbiota-related lipid metabolism and amino acid metabolism [40]. The active peptide of Walker ameliorated hyperlipidemia by altering amino acid metabolism [41]. In addition, *B. pseudolongum* prevented liver injury in mice by regulating the gut microbiota composition and liver metabolites-related phenylalanine metabolism, and alanine, citrate cycle, and so on [42]. These results were similar to our study.

In addition, *B. pseudolongum* and *B. animalis* had a positive correlation with deoxycholic acid, xanthosine, and cholesterol sulfate and had a negative correlation with these metabolites from amino acid metabolism, while *Helicobacter hepaticus*, *Rothia mucilaginosa,* and *Clostridium celatum* were in reverse. *Helicobacter hepaticus*, *Rothia mucilaginosa*, and *Clostridium celatum* might promote amino acid metabolism. Tamarind xyloglucan oligosaccharides

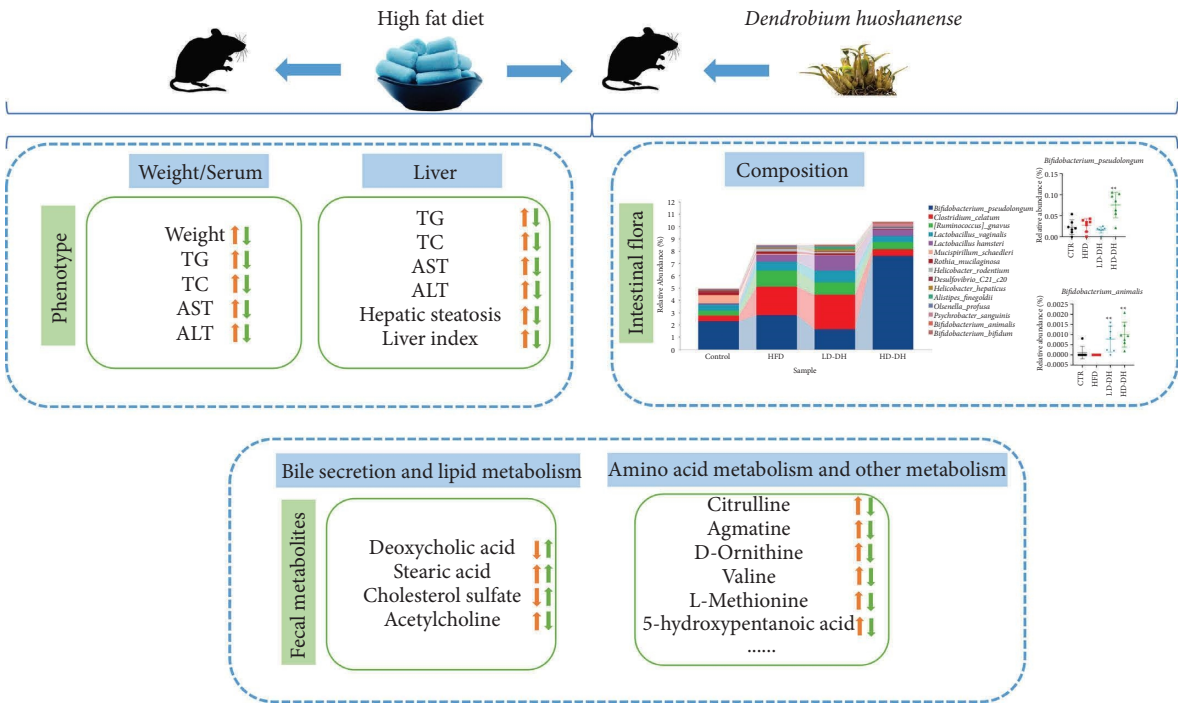

Figure 9: Effects of DH in the mice with lipid metabolism disorders. The pink and green arrows correspond to the HFD and HD-DH groups, respectively. The upward arrows indicate upregulation effects and the downward arrows represent downregulation effects.

treatment promoted the proliferation the *B. pseudolongum* and reduced the abundance of opportunistic pathogen species and attenuated metabolic disorders [43]. *B. pseudolongum* and *B. animalis* enriched by DH might suppress amino acid metabolism by inhibiting the growth of harmful bacteria, such as *Helicobacter hepaticus*, *Rothia mucilaginosa,* and *Clostridium celatum.*

In this study, Pearson's correlation analysis showed that DH might directly enhance the excretion of deoxycholic acid, stearic acid, and cholesterol sulfate, as well as alter amino acid metabolism and other pathway metabolism, to lower the levels TG and TC and regulate lipid metabolism via the metabolic ability of the gut flora.

5. Conclusion

DH treatment was found to reduce lipid levels and improve liver function in HFD mice. DH most likely exerts an antihyperlipidemic effect by shaping the intestinal flora and its metabolites, which are closely related to lipid metabolism (Figure 9). Thus, this study provides evidence that DH, a traditional medicinal and edible herb, may be an important candidate for preventing and improving lipid metabolism by regulating the gut flora. In the future, the clinical efficacy of DH in improving lipid metabolism disorders will need to be evaluated for the development and utilization of DH.

Data Availability

The data used to support the findings of the study are available upon reasonable request from the corresponding author.

Conflicts of Interest

The authors declare that this study was conducted in the absence of any commercial or financial relationships that could be construed as conflicts of interest.

Authors' Contributions

MM and FG performed the experiments. MM, CC, QL, KH, and XL performed the experiments. MM drafted the manuscript. LG, YJ, and JD reviewed the manuscript. BH conceived the study. Menghua Ma and Fangli Gu contributed equally to this work.

Acknowledgments

We are grateful to Shanghai Personalbio Technology Co. Ltd. and Suzhou PANOMIX Biomedical Tech Co. Ltd. for their technical support with 16S rRNA gene sequencing and untargeted metabolomic analyses, respectively. This work was supported by the Major Science and Technology Projects of Anhui Province (Grant no. 202003a070220003), Scientific and Technological Innovation Project of China Academy of Chinese Medical Sciences (Grant no. CI2021B013), China Agriculture Research System of MOF and MARA (Grant no. CARS-21), High Level Talents Scientific Research Startup Fund of 2021 at West Anhui University (Grant no. WGKQ2021081), Fund of Traditional Chinese Medicine Institute of Anhui Dabie Mountain (Grant no. TCMADM-2023-01), the Key Project of Natural Science Research in Universities in Anhui Province (Grant no. KJ2021A0957), West Anhui University (Grant no.

WXZR201935), and Anhui Provincial Department of Education Excellent Top Talents Cultivation Project for Universities (Grant no. gxgnfx2021144).

References

[1] M. Liu, W. Shi, Y. Huang, Y. Wu, and K. Wu, "Intestinal flora: a new target for traditional Chinese medicine to improve lipid metabolism disorders," *Frontiers in Pharmacology*, vol. 14, Article ID 1134430, 2023.

[2] K. Guo, C. Figueroa-Romero, M. Noureldein et al., "Gut microbiota in a mouse model of obesity and peripheral neuropathy associated with plasma and nerve lipidomics and nerve transcriptomics," *Microbiome*, vol. 11, no. 1, p. 52, 2023.

[3] H. Wang, P. Dong, X. Liu et al., "Active peptide AR-9 from eupolyphaga sinensis reduces blood lipid and hepatic lipid accumulation by restoring gut flora and its metabolites in a high fat diet-induced hyperlipidemia rat," *Frontiers in Pharmacology*, vol. 13, Article ID 918505, 2022.

[4] A. Li, J. Wang, Y. Wang et al., "Tartary buckwheat (fagopyrum tataricum) ameliorates lipid metabolism disorders and gut microbiota dysbiosis in high-fat diet-fed mice," *Foods*, vol. 11, no. 19, p. 3028, 2022.

[5] L. Li, W. Guo, W. Zhang et al., "Grifola frondosa polysaccharides ameliorate lipid metabolic disorders and gut microbiota dysbiosis in high-fat diet fed rats," *Food and Function*, vol. 10, no. 5, pp. 2560–2572, 2019.

[6] T. Li, H. Teng, F. An, Q. Huang, L. Chen, and H. Song, "The beneficial effects of purple yam (Dioscorea alata L.) resistant starch on hyperlipidemia in high-fat-fed hamsters," *Food & Function*, vol. 10, no. 5, pp. 2642–2650, 2019.

[7] G. Zhu, F. Ma, G. Wang et al., "Bifidobacteria attenuate the development of metabolic disorders, with inter- and intra-species differences," *Food & Function*, vol. 9, no. 6, pp. 3509–3522, 2018.

[8] Z. Zhang, Y. Wang, Y. Zhang et al., "Synergistic effects of the jackfruit seed sourced resistant starch and Bifidobacterium pseudolongum subsp. globosum on suppression of hyperlipidemia in mice," *Foods*, vol. 10, no. 6, p. 1431, 2021.

[9] T. Bo, J. Wen, Y. Zhao, S. Tian, X. Zhang, and D. Wang, "Bifidobacterium pseudolongum reduces triglycerides by modulating gut microbiota in mice fed high-fat food," *The Journal of Steroid Biochemistry and Molecular Biology*, vol. 198, Article ID 105602, 2020.

[10] Y. Huo, G. Zhao, J. Li et al., "Bifidobacterium animalis subsp. lactis A6 enhances fatty acid β-oxidation of adipose tissue to ameliorate the development of obesity in mice," *Nutrients*, vol. 14, no. 3, p. 598, 2022.

[11] Y. Tian, J. Cai, W. Gui et al., "Berberine directly affects the gut microbiota to promote intestinal farnesoid X receptor activation," *Drug Metabolism and Disposition*, vol. 47, no. 2, pp. 86–93, 2019.

[12] A. Bordoni, A. Amaretti, A. Leonardi et al., "Cholesterol-lowering probiotics: in vitro selection and in vivo testing of bifidobacteria," *Applied Microbiology and Biotechnology*, vol. 97, no. 18, pp. 8273–8281, 2013.

[13] F. Xu, X. Hu, W. Singh, W. Geng, I. Tikhonova, and J. Lin, "The complex structure of bile salt hydrolase from Lactobacillus salivarius reveals the structural basis of substrate specificity," *Scientific Reports*, vol. 9, no. 1, Article ID 12438, 2019.

[14] L. Gao, F. Wang, T. Hou et al., "Dendrobium huoshanense C.Z.Tang et S.J.Cheng: a Review of Its Traditional Uses, Phytochemistry, and Pharmacology," *Frontiers in Pharmacology*, vol. 13, Article ID 920823, 2022.

[15] X. Zha, H. Zhao, V. Bansal, L. Pan, Z. Wang, and J. Luo, "Immunoregulatory activities of Dendrobium huoshanense polysaccharides in mouse intestine, spleen and liver," *International Journal of Biological Macromolecules*, vol. 64, pp. 377–382, 2014.

[16] H. Ye, Z. Shang, F. Zhang, X. Zha, Q. Li, and J. Luo, "Dendrobium huoshanense stem polysaccharide ameliorates alcohol-induced gastric ulcer in rats through Nrf2-mediated strengthening of gastric mucosal barrier," *International Journal of Biological Macromolecules*, vol. 236, Article ID 124001, 2023.

[17] Q. Li, X. Yang, X. Zha et al., "Protective effects of three flavonoids from dendrobium huoshanense flowers on alcohol-induced hepatocyte injury via activating Nrf2 and inhibiting NF-κB pathways," *Chemistry and Biodiversity*, vol. 19, no. 8, Article ID e202200471, 2022.

[18] X. Fan, J. Han, L. Zhu et al., "Protective Activities of *Dendrobium huoshanense* C. Z. Tang et S. J. Cheng Polysaccharide against High-Cholesterol Diet-Induced Atherosclerosis in Zebrafish," *Oxidative Medicine and Cellular Longevity*, vol. 2020, Article ID 8365056, 12 pages, 2020.

[19] X. Wang, J. Luo, R. Chen, X. Zha, and L. Pan, "Dendrobium huoshanense polysaccharide prevents ethanol-induced liver injury in mice by metabolomic analysis," *International Journal of Biological Macromolecules*, vol. 78, pp. 354–362, 2015.

[20] S. Xie, B. Liu, H. Ye et al., "Dendrobium huoshanense polysaccharide regionally regulates intestinal mucosal barrier function and intestinal microbiota in mice," *Carbohydrate Polymers*, vol. 206, pp. 149–162, 2019.

[21] Y. Liang, J. Han, and M. Yu, "Dendrobium Huoshanense C. Z. Tang et S. J. Cheng inhibits the development of atherosclerosis and vascular calcification induced by high-fat diet in LDLR-/- mice," *Chinese Journal of Arteriosclerosis*, vol. 28, no. 11, pp. 930–935, 2020.

[22] J. Zhang, C. Lian, and Y. Lin, "The effect of dendrobium huoshenese capsule on blood lipid and lipoperoxidation in the hyperlipidemic rats," *Acta Laser Biology Sinica*, vol. 19, no. 5, pp. 628–633, 2010.

[23] N. Vasilev, J. Boccard, G. Lang et al., "Structured plant metabolomics for the simultaneous exploration of multiple factors," *Scientific Reports*, vol. 6, no. 1, Article ID 37390, 2016.

[24] E. Zelena, W. Dunn, D. Broadhurst et al., "Development of a robust and repeatable UPLC-MS method for the long-term metabolomic study of human serum," *Analytical Chemistry*, vol. 81, no. 4, pp. 1357–1364, 2009.

[25] E. Want, P. Masson, F. Michopoulos et al., "Global metabolic profiling of animal and human tissues via UPLC-MS," *Nature Protocols*, vol. 8, no. 1, pp. 17–32, 2013.

[26] F. Koubaa-Ghorbel, M. Chaâbane, M. Turki, F. Makni-Ayadi, and A. El Feki, "The protective effects of Salvia officinalis essential oil compared to simvastatin against hyperlipidemia, liver, and kidney injuries in mice submitted to a high-fat diet," *Journal of Food Biochemistry*, vol. 44, no. 4, Article ID e13160, 2020.

[27] L. Yu, R. Gao, X. Song, X. Li, and J. Zhu, "Cardio-protective and anti-atherosclerosis effect of crocetin on vitamin D3 and HFD-induced atherosclerosis in rats," *Journal of Oleo Science*, vol. 70, no. 10, pp. 1447–1459, 2021.

[28] X. Li, N. Deng, T. Zheng et al., "Importance of Dendrobium officinale in improving the adverse effects of high-fat diet on

mice associated with intestinal contents microbiota," *Frontiers in Nutrition*, vol. 9, Article ID 957334, 2022.

[29] X. Li, X. Peng, K. Guo, and Z. Tan, "Bacterial diversity in intestinal mucosa of mice fed with Dendrobium officinale and high-fat diet," *3 Biotech*, vol. 11, no. 1, p. 22, 2021.

[30] T. Lan, Y. Yu, J. Zhang et al., "Cordycepin ameliorates nonalcoholic steatohepatitis by activation of the AMP-activated protein kinase signaling pathway," *Hepatology*, vol. 74, no. 2, pp. 686–703, 2021.

[31] K. Mao, J. Gao, X. Wang et al., "Bifidobacterium animalis subsp. lactis BB-12 has effect against obesity by regulating gut microbiota in two phases in human microbiota-associated rats," *Frontiers in Nutrition*, vol. 8, Article ID 811619, 2021.

[32] A. Chen, T. Fang, H. Ho et al., "A multi-strain probiotic blend reshaped obesity-related gut dysbiosis and improved lipid metabolism in obese children," *Frontiers in Nutrition*, vol. 9, Article ID 922993, 2022.

[33] H. Lv, F. Tao, L. Peng et al., "In vitro probiotic properties of Bifidobacterium animalis subsp. lactis SF and its alleviating effect on non-alcoholic fatty liver disease," *Nutrients*, vol. 15, no. 6, p. 1355, 2023.

[34] S. Weninger, C. Herman, R. Meyer et al., "Oligofructose improves small intestinal lipid-sensing mechanisms via alterations to the small intestinal microbiota," *Microbiome*, vol. 11, no. 1, p. 169, 2023.

[35] Y. Yue, Y. Wang, Q. Xie et al., "*Bifidobacterium bifidum* E3 combined with *Bifidobacterium longum subsp. infantis* E4 improves LPS-induced intestinal injury by inhibiting the TLR4/NF-κB and MAPK signaling pathways *in vivo*," *Journal of Agricultural and Food Chemistry*, vol. 71, no. 23, pp. 8915–8930, 2023.

[36] J. Ji, S. Zhang, M. Yuan et al., "Fermented rosa roxburghii tratt juice alleviates high-fat diet-induced hyperlipidemia in rats by modulating gut microbiota and metabolites," *Frontiers in Pharmacology*, vol. 13, Article ID 883629, 2022.

[37] X. Liang, Z. Zhang, X. Zhou et al., "Probiotics improved hyperlipidemia in mice induced by a high cholesterol diet via downregulating FXR," *Food & Function*, vol. 11, no. 11, pp. 9903–9911, 2020.

[38] Y. Song, D. Lu, H. Wang et al., "Metagenomic insights into the anti-obesity effect of a polysaccharide from saccharina japonica," *Foods*, vol. 12, no. 3, p. 665, 2023.

[39] A. Lake, P. Novak, P. Shipkova et al., "Branched chain amino acid metabolism profiles in progressive human nonalcoholic fatty liver disease," *Amino Acids*, vol. 47, no. 3, pp. 603–615, 2015.

[40] Y. Guo, M. Liu, X. Liu et al., "Metagenomic and untargeted metabolomic analysis of the effect of sporisorium reilianum polysaccharide on improving obesity," *Foods*, vol. 12, no. 8, p. 1578, 2023.

[41] Y. Li, P. Dong, L. Dai, and S. Wang, "Untargeted and targeted metabolomics reveal the active peptide of eupolyphaga sinensis walker against hyperlipidemia by modulating imbalance in amino acid metabolism," *Molecules*, vol. 28, pp. 7049–7120, 2023.

[42] W. Guo, S. Cui, X. Tang et al., "Intestinal microbiomics and hepatic metabolomics insights into the potential mechanisms of probiotic Bifidobacterium pseudolongum CCFM1253 preventing acute liver injury in mice," *Journal of the Science of Food and Agriculture*, vol. 103, no. 12, pp. 5958–5969, 2023.

[43] C. Zhu, Y. Li, Y. Xu, N. Wang, Q. Yan, and Z. Jiang, "Tamarind xyloglucan Oligosaccharides attenuate metabolic disorders via the gut-liver Axis in mice with high-fat-diet-induced obesity," *Foods*, vol. 12, no. 7, p. 1382, 2023.